Magnetic properties of Mn-doped 6*H*-SiC

Bo Song,[1,2] Huiqiang Bao,[1] Hui Li,[1] Ming Lei,[1] Jikang Jian,[3] Jiecai Han,[4] Xinghong Zhang,[4] Songhe Meng,[4] Wanyan Wang,[1] and Xiaolong Chen[1,a)]

[1]*Beijing National Laboratory for Condensed Matter Physics, Institute of Physics, Chinese Academy of Sciences, P.O. Box 603, Beijing 100190, People's Republic of China*

[2]*Academy of Fundamental and Interdisciplinary Sciences, Harbin Institute of Technology, Harbin 150080, People's Republic of China*

[3]*Department of Physics, Xinjiang University, Urumchi 830046, People's Republic of China*

[4]*Center for Composite Materials, Harbin Institute of Technology, Harbin 150080, People's Republic of China*

(Received 28 November 2008; accepted 19 February 2009; published online 11 March 2009)

We report the synthesis and characterizations of low Mn-doped ($<10^{-3}$ molar fraction) 6*H*-SiC. Raman scattering studies show an unusual shift in Raman peak with altering Mn contents. The magnetic properties measurement shows the typical ferromagnetic order was established at as low Mn-doped concentration as 10^{-4} molar fraction at around 250 K. It is speculated that the defects-related effects other than the Mn content play a more important role to determine the magnetic ordering. © *2009 American Institute of Physics*. [DOI: 10.1063/1.3097809]

Owing to its potential applications in spintronics, diluted magnetic semiconductors (DMSs) have been investigated extensively over past years since Dietl *et al.*[1] predicted the existence of room temperature (RT) ferromagnetic (FM) in transition metal (TM) doped semiconductors, such as in GaN,[2] ZnO,[3–5] and GaAs,[6] etc. Recently, wide band-gap semiconductor SiC (3.03 eV for 6*H*-SiC) has attracted much attention as promising DMSs. A series of SiC:TM (TM =Mn, Fe, Co, Cr, etc.) have been synthesized and investigated by several research groups.[7–14] For DMSs, such as SiC:TM, there still exist two challenges: (1) the realization of Curie temperature (T_c) around or above RT; (2) whether the obtained material is indeed a solid solution of $Si_{1-x}TM_xC$ or it remains as SiC matrix with embedded TM clusters, precipitates, or second phases that are responsible for the observed magnetic properties. Toward this role, more efforts are required.

Raman scattering is a convenient spectroscopic technique to characterize samples: nondestructive and contactless.[15] The variations in Raman peak linewidths and frequencies could be interpreted by anharmonic crystal field theory and provides useful information to know the carrier-phonon interaction.[4]

In this letter, we synthesized a series of low Mn-doped ($<1\times10^{-3}$ molar fraction) SiC samples and found similar FM transitions at ~250 K as reported by Ma *et al.*[8] in polycrystalline bulk $Si_{1-x}Mn_xC(x\geq0.01)$. Raman frequency and linewidths exhibited an abnormal behavior with the altering of Mn content. The observation of T_c at ~250 K in such low Mn content doped SiC suggests that the Mn doping content is not vital to determine the T_c of SiC:Mn.

Mn-doped SiC was prepared by high-purity silicon (99.999%), carbon (99.999%, graphite) and manganese (99.999%) powder. The reaction process follows the similar route as described in Ref. 11.

Figure 1 shows the x-ray diffraction (XRD) pattern of $Si_{1-x}Mn_xC$ with $x=2.4\times10^{-4}$, 5×10^{-4}, and 1×10^{-3}, determined by inductively coupled plasma-atomic emission spectrometry, and defined as M_1, M_2, and M_3, respectively. It is evident that only the peaks corresponding to 6*H*-SiC (ICDD-PDF: 29–1131), 15R-SiC (ICDD-PDF: 39–1196), and trace impurity phase of carbon (ICDD-PDF: 26–1079) exist within the sensitivity of XRD diffractometer (Philips X'PERT MPD). Mn as an impurity element disturbs the phase equilibrium and induces the formation of 15R-SiC. The evolution of cell

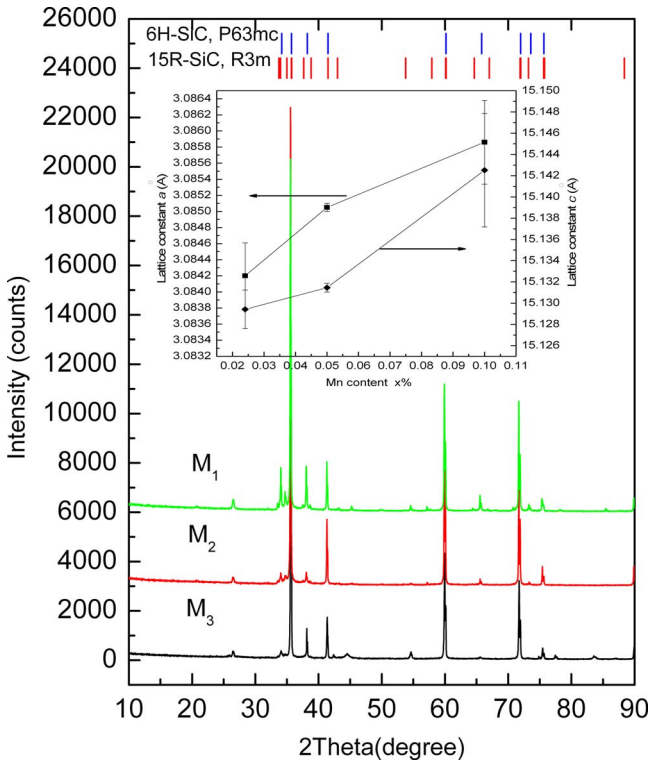

FIG. 1. (Color online) XRD pattern of M_1, M_2, and M_3. Vertical bars at the top are expected Bragg positions for 6*H*-SiC and 15R-SiC. Inset: the evolution of cell parameters a and c of $Si_{1-x}Mn_xC$ as a function of Mn content x.

a)Author to whom correspondence should be addressed. Electronic mail: chenx29@aphy.iphy.ac.cn. Tel.: +86-10-82649039. FAX: +86-10-82649646.

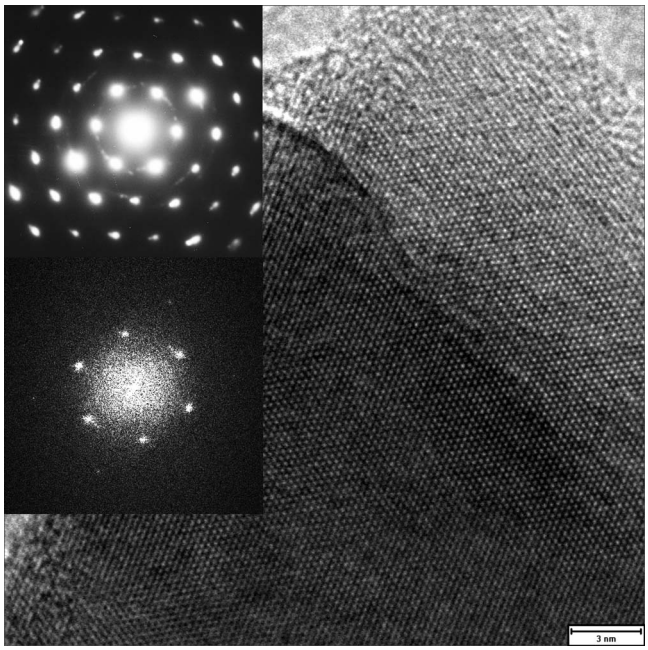

FIG. 2. M_3, that is HRTEM image of M_3. Top inset is the SAED pattern and bottom inset is the FFT image of M_3.

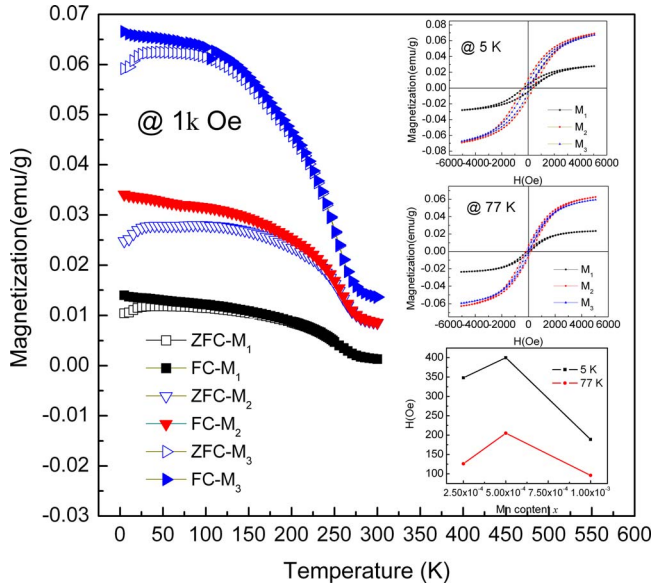

FIG. 4. (Color online) Temperature dependence of the FC and ZFC at 1kOe for M_1, M_2, and M_3. Top inset: the magnetization loops for M_1, M_2, and M_3 at 5 K. Middle inset: the magnetization loops for M_1, M_2, and M_3 at 77 K. Bottom inset shows the H_c as a function of Mn content at 5 K and 77 K, respectively.

parameters a and c with Mn content x is shown in the inset of Fig. 1 as filled squares and diamond, respectively. Both a and c increase slightly with the increment in x. Figure 2 shows the high-resolution transmission electron microscopy (HRTEM) image taken randomly on the particles from M_3. Clear lattice fringes suggest a good crystallinity. Selected area electron diffraction (SAED) pattern (top inset) and fast Fourier transform (FFT) image (bottom inset) reveals the single crystal nature of particles. Similar results are obtained in the cases of M_1 and M_2.

The RT Raman spectra were shown in Fig. 3. For simplicity, the spectrometer response function was not taken into account, and frequencies and linewidths [full widths at half maximum (FWHM)] for the optical phonons modes were

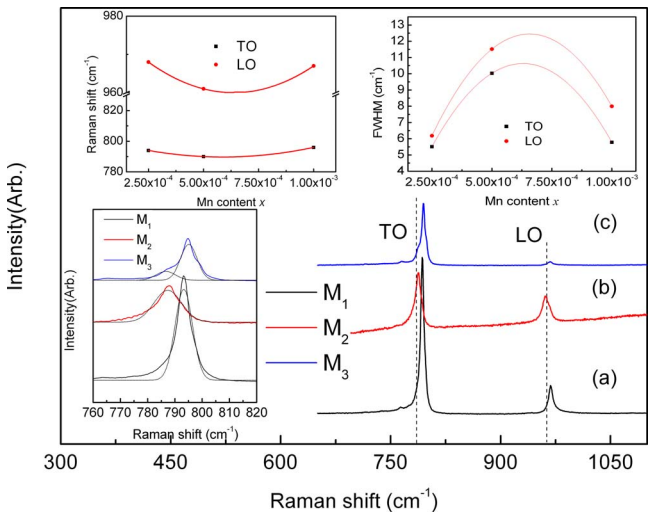

FIG. 3. (Color online) Raman spectra of Mn-doped SiC particles (a) M_1, (b) M_2, and (c) M_3. Top-left inset: the phonon frequencies of TO and LO modes as a function of Mn content. Top-right inset: FWHM of TO and LO modes as a function of Mn content. Curves through the data in these two insets are guides for the eyes. Bottom-left inset: the Lorentzian function fit of the TO modes.

fitted by using a Lorentzian function as shown in the bottom-left inset. In Fig. 3, the strongest and sharpest peak at $\sim 794\ \mathrm{cm}^{-1}(M_1)$ was assigned to the transverse-optical (TO) mode of 6*H*-SiC, and the peak at $\sim 967\ \mathrm{cm}^{-1}(M_1)$ corresponded to the longitudal-optical (LO) mode.[16] The frequency variations in LO and TO modes as a function of x were plotted in the top-left inset. The Raman peaks shift to low frequency with the increment in x ($x \leq 5 \times 10^{-4}$) and then turn to high frequency with x is further increased to 10^{-3}. It is well known that the LO-phonon-plasmon coupling effect usually appear in undoped n-type semiconductor, such as InN (Ref. 17) and GaAs.[18] For the case of SiC, it is speculated that a similar mechanism is still true. Mn is an effective trap in wide band-gap semiconductors.[19] It can capture and reduce free carrier concentrations (n_c) that will lower the frequency of both upper and lower branches of coupled modes and Raman peak; thus shifts to low frequency with the increment in x ($x \leq 5 \times 10^{-4}$). With the further increasing of x, p-type carrier may dominate as Mn is probably amphoteric. The coupled modes were thus enhanced with the Raman peak shifting to high frequency, as shown in inset of Fig. 3. The FWHM (top-right inset) for TO mode increases from 5.48 to 10.01 cm^{-1} with the increment in x ($x \leq 5 \times 10^{-4}$). For M_3, TO phonon line shape could be fitted by two independent peaks (bottom-left inset in Fig. 3). The reason for the appearance of the shoulder peak is unclear and need further investigation.

Figure 4 shows the temperature dependence of zero field cooled (ZFC) and FC magnetization curves (M-T) at 1kOe. The smooth M-T curve indicates the absence of additional magnetic phase. From Fig. 4, it can be seen clearly that for all Mn-doped 6*H*-SiC samples, M-T curves exhibit a similar magnetic phase transition from FM to paramagnetic phase at ~ 250 K. Magnetization versus magnetic field (M-H) curves of all samples at 5 and 77 K are shown in top and middle inset of Fig. 4, respectively. The well-defined hysteresis loops indicate the robust FM ordering dominated the sample.

Similar results have been reported in several Mn-doped SiC systems, including bulk pellets, thin films, and powder form sample as well.[7–9] That is to say, the FM behavior in Mn-doped SiC may be not dependent on its shape (film or particle) but the synthesis conditions may serve as the key role to affect the magnetic properties. Compared with M_1 and M_2 (bottom inset in Fig. 4), M_3 exhibits a reduced coercive field (H_c) due to the possible enhanced antiferromagnetic (AFM) component which intensified the competition with FM interaction as x is increased.

To investigate the FM origin, we first take into account the purity of starting materials. The most convincing evidence against the impurity effect is all the pristine, that is, neither silicon, carbon, nor manganese powder exhibited FM signals. The absence of any secondary magnetic phase, as confirmed by M-T and HRTEM studies, has ruled out the possibility of FM due to extrinsic origin. Even if some tiny parasitic phase was not detected, the FM signal cannot be ascribed to the impurity magnetic phase since nearly all possible Mn–C and Mn–Si compounds are all non-FM except Mn_4Si_7 with $T_c \sim 30$ K and MnSi with $T_c \sim 47$ K.[20,21] Since only trace Mn was introduced to SiC, the large Mn–Mn distance make the direct interaction impossible to occur. Furthermore, the carrier-mediated indirect Ruderman–Kittel–Kasuya–Yosida exchange interaction will also not work due to the low n_c. Recently, the donor impurity band exchange model proposed by Coey *et al.*[22] was thought to be responsible for high-resistivity samples with the n_c larger than 10^{20} cm^{-3}.[23] However, the n_c, for the case of M_1, is calculated to be for $\sim 1.2 \times 10^{19}$ cm^{-3}. Obviously, it also failed to result in FM order. Recently, defects are found to play a decisive role to connect the localized spins and induce FM order in undoped systems,[24,25] such as III-V nitrides.[26] Thus, it is speculated the defects also have great contribution for FM order in Mn-doped SiC. Compared with Ref. 8, 40 times less in Mn content still realize a similar T_c and effective magnetic moment μ_{eff} in Mn-doped SiC, suggesting the defects and disorder rather than Mn content serves a key role to induce long-range magnetic order. Only in such case, the superlow Mn content provides the defects an opportunity to display their possible contribution for FM. This study will urge an effort to reinvestigate the magnetic properties of SiC:TM since the role of defects was not taken into consideration in previous studies. However, more detailed research is still required to investigate the nature FM origin in Mn-doped SiC.

In conclusion, Mn-doped SiC with good crystallinity was obtained. Raman measurements showed an unusual shift in Raman peaks with the increasing of Mn content. It found that the FM order may not be dependent on the Mn doping content, but the defects may serve as the key role.

This work is supported by 2008 Ludo Frevel Crystallography Scholarship Award. China Postdoctoral Science Foundation funded project, and Development Program for Outstanding Young Teachers in Harbin Institute of Technology (HIT).

[1] T. Dietl, H. Ohno, F. Matsukura, J. Cibert, and D. Ferrand, Science **287**, 1019 (2000).
[2] K. Biswas, K. Sardar, and C. N. R. Rao, Appl. Phys. Lett. **89**, 132503 (2006).
[3] H. S. Hsu, J. C. A. Huang, S. F. Chen, and C. P. Liu, Appl. Phys. Lett. **90**, 102506 (2007).
[4] J. B. Wang, G. J. Huang, X. L. Zhong, L. Z. Sun, Y. C. Zhou, and E. H. Liu, Appl. Phys. Lett. **88**, 252502 (2006).
[5] S. K. Mandal, A. K. Das, T. K. Nath, and D. Karmakar, Appl. Phys. Lett. **89**, 144105 (2006).
[6] H. Ohno, A. Shen, F. Matsukura, A. Oiwa, A. Endo, S. Katsumoto, and Y. Iye, Appl. Phys. Lett. **69**, 363 (1996).
[7] W. H. Wang, F. Takanoa, H. Ofuchib, and H. Akinaga, J. Magn. Magn. Mater. **310**, 2141 (2007).
[8] S. B. Ma, Y. P. Sun, B. C. Zhao, P. Tong, X. B. Zhu, and W. H. Song, Physica B **394**, 122 (2007).
[9] N. Theodoropoulou, A. F. Hebard, S. N. G. Chu, M. E. Overberg, C. R. Abernathy, S. J. Pearton, R. G. Wilson, J. M. Zavada, and Y. D. Park, J. Vac. Sci. Technol. A **20**, 579 (2002).
[10] I. Kuryliszyn-Kudelska, R. Diduszko, E. Tymicki, W. Dobrowolski, and K. Grasza, Phys. Status Solidi B **244**, 1743 (2007).
[11] B. Song, J. K. Jian, H. Li, M. Lei, H. Q. Bao, X. L. Chen, and G. Wang, Physica B **403**, 2897 (2008).
[12] M. S. Miao and W. R. L. Lambrecht, Phys. Rev. B **74**, 235218 (2006).
[13] M. S. Miao and W. R. L. Lambrecht, Phys. Rev. B **68**, 125204 (2003).
[14] M. S. Miao and W. R. L. Lambrecht, Phys. Rev. B **71**, 214405 (2005).
[15] B. Song, J. K. Jian, G. Wang, H. Q. Bao, and X. L. Chen, J. Appl. Phys. **101**, 124302 (2007).
[16] M. Hofmann, A. Zywietz, K. Karch, and F. Bechstedt, Phys. Rev. B **50**, 13401 (1994).
[17] B. Song, J. K. Jian, G. Wang, Z. H. Zhang, M. Lei, H. Q. Bao and X. L. Chen, Physica E (Amsterdam) **40**, 579 (2008).
[18] A. Kasic, M. Schubert, Y. Saito, Y. Nanishi, and G. Wagner, Phys. Rev. B **65**, 115206 (2002).
[19] H. Li, H. Q. Bao, B. Song, W. J. Wang, X. L. Chen, L. J. He, and W. X. Yuan, Physica B **403**, 4096 (2008).
[20] M. Yamada, T. Goto, and T. Kanomata, J. Alloys Compd. **364**, 37 (2004).
[21] J. J. Hauser, Phys. Rev. B **22**, 2554 (1980).
[22] J. M. D. Coey, M. Venkatesan, and C. B. Fitzgerald, Nature Mater. **4**, 173 (2005).
[23] K. Ueda, H. Tabata, and T. Kawai, Appl. Phys. Lett. **79**, 988 (2001).
[24] C. Madhu, A. Sundaresan, and C. N. R. Rao, Phys. Rev. B **77**, 201306(R) (2008).
[25] B. Song, H. Q. Bao, H. Li, M. Lei, T. H. Peng, J. K. Jian, J. Liu, W. Y. Wang, W. J. Wang, and X. L. Chen, J. Am. Chem. Soc. **131**, 1376 (2009).
[26] P. Dev, Y. Xue, and P. Zhang, Phys. Rev. Lett. **100**, 117204 (2008).